ACS APPLIED MATERIALS & INTERFACES

Research Article

www.acsami.org

Fluorescent Cross-Linked Polystyrene Perylenebisimide/ Oligo(*p*-Phenylenevinylene) Microbeads with Controlled Particle Size, Tunable Colors, and High Solid State Emission

Swapnil L. Sonawane and S. K. Asha*

Polymer & Advanced Material Laboratory, Polymer Science & Engineering Division, CSIR- NCL, Pune-411008, Maharashtra, India

Supporting Information

ABSTRACT: A series fo cross-linked fluorescent polystyrene (PS) microbeads with narrow size distribution and intense solid state emission was developed. Fluorophores based on perylene bisimide (**PBI**) and oligo(*p*-phenylenevinylene) (**OPV**) designed as acrylic cross-linkers were introduced into the polymerization recipe in a two-stage dispersion polymerization, carried out in ethanol in the presence of poly(vinylpyrrolidone) (PVP) as stabilizer. The structural design permitted introduction of up to 10^{-5} moles of the fluorophores into the polymerization medium without fouling of the dispersion. The particle size measured using dynamic light scattering (DLS) indicated that they were nearly monodisperse with size in the range 2−3 μm depending on the amount of fluorophore incorporated. Fluorescence microscope images of ethanol dispersion of the sample exhibited intense orange red emission for **PS-PBI-X** series and green emission for **PS-OPV-X** series. A PS incorporated with both **OPVX** and **PBIX** exhibited dual emission upon exciting at the OPV wavelength of 350 nm and PBI wavelength of 490 nm, respectively. The low incorporation of fluorophore resulted in almost complete absence of aggregation induced reduction in fluorescence as well as red-shifted aggregate emission. The solid state emission quantum yield measured using integrating-sphere setup indicated a very high quantum yield of ϕ_{powder} = 0.71 for **PS-OPV-X** and ϕ_{powder} = 0.25 for **PS-PBI-X** series. The cross-linked PS microbeads incorporating both OPV and PBI chromophores had a ϕ_{powder} = 0.33 for PBI emission and ϕ_{powder} = 0.20 for OPV emission. This strategy of introducing fluorophore as cross-linkers into the PS backbone is very versatile and amenable to simultaneous addition of different suitably designed fluorophores emitting at different wavelengths.

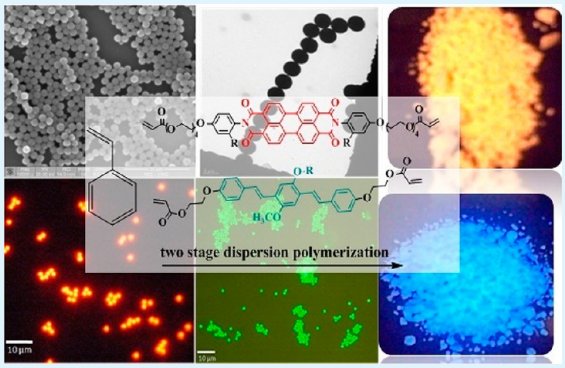

KEYWORDS: *fluorescent cross-linker, perylenebisimide, oligo(p-phenylenevinylene), dispersion polymerization, dual emission, solid state fluorescence*

INTRODUCTION

Fluorescent polymer beads find application in myriad areas like multicolor emission,[1] bar-coding,[2] photonic crystals,[3] and self-assembly study[4] and as a standard in the fluorescence techniques like flow cytometry,[5] cell sorting,[6] sensing and imaging, etc.[7−9] Some of the important criteria for application of the fluorescent beads are monodispersity, nonleaching of the fluorophore, thermal and photostability, etc.[10,11]Although fluorescent microspheres are commercially available their prohibitive cost as well as limited choice of the emission colors makes it important to design efficient fluorescent microspheres with narrow size distribution and a wide range of emission color using easily adaptable procedure in the laboratory as well as in the industry. Fluorescent polymer particles are generally synthesized by incorporation of the dye with the polymer composite, physical adsorption,[12] encapsulation of the dye in block copolymers by hydrophobic−hydrophilic interaction,[13−15] gradual solvent evaporation,[16] controlled mixing,[17] and so on.[18,19] However these methods often face the problem of the dye leakage causing background fluorescence interference. The fluorescent polymer particles can also be synthesized by postpolymerization dispersion techniques. However, these systems require additional steps after polymerization and control over uniform emission, and monodispersity of the polymer particle is also difficult. To overcome these problems, copolymerization with polymerizable fluorophore and covalently attaching the fluorophore to the polymer chains is a good means to prevent leakage and obtain strongly fluorescent polymer particle with uniform distribution of the fluorophore in the polymer backbone.[20−22] A polymerization methodology has also to be adopted which would allow for narrow size distribution of the fluorophore incorporated polymer.

Received: October 4, 2013
Accepted: November 5, 2013
Published: November 5, 2013

   dx.doi.org/10.1021/am404354q | *ACS Appl. Mater. Interfaces* 2013, 5, 12205−12214

Various polymerization techniques like suspension,[23] emulsion,[24] dispersion,[25,26] etc. are utilized to obtain narrow disperse polymer beads in size ranges varying from nanometer to micrometer depending on the size requirement for different applications. Among these methods, dispersion polymerization is a very attractive one for the large-scale preparation of nearly monodisperse polymer beads in the 0.5−15 μm size range. The original dispersion polymerization method as developed in the early 1960s did not facilitate the incorporation of fluorophores, functional comonomers, cross-linkers, etc.[25] In the presence of these "extra" reagents the polymerization would lose control over particle size and especially with cross-linkers result in coagulation of the polymer. In the early 2000s, M. A. Winnik et al. showed that polymer beads with narrow size distribution could be achieved in the dispersion polymerization method by delayed introduction of the cross-linker after the nucleation stage, which they named as the "two-stage" dispersion polymerization.[27,28] Using this procedure they demonstrated the successful incorporation of up to 3 mol % of the cross-linker divinyl benzene (DVB) into PS and still obtained nearly monodisperse particles.

In this report we present the incorporation of fluorescent cross-linkers into a commercially available polymer like that of polystyrene (PS), adopting a two-stage dispersion polymerization route to produce highly fluorescent nearly monodisperse PS beads. Among various commercially available polymers, polystyrene affords good control over the particle size, and fluorescently labeled PS beads are compatible as cell markers for tracing both in vivo and in vitro.[8] Among stable organic fluorophores which have high quantum efficiency, perylene 3,4,9,10-tetracarboxylic diimide (PBI) and oligo(*p*-phenylenevinylene) (OPV) are some of the most preferred due to their strong absorption and fluorescence quantum yield combined with outstanding chemical, thermal, and photochemical stability.[29−32] We report new cross-linkers based on perylene 3,4,9,10-tetracarboxylic diimide (PBI) and oligo(*p*-phenylenevinylene) (OPV) known for their high quantum efficiency, which were made more compatible with the dispersion polymerization recipe by the introduction of flexible groups like tetraethylene glycol or branched alkoxy units. The fluorescent polystyrene beads were analyzed using microscopic techniques like fluorescence microscopy, scanning electron microscopy (SEM), and transmission electron microscopy (TEM). Photophysical characterization was carried out using absorption and fluorescence spectroscopic techniques. Using this methodology of fluorophore as the cross-linker it was observed that as few as 10^{-7} moles of the fluorophore was sufficient to obtain highly fluorescent polystyrene beads which retained their high emission in the solid powder state (ϕ_{powder} = 0.71%) also. The specific issues that are highlighted in this work are as follows:

(a) An easy and scalable route toward thermally stable fluorescent monodisperse cross-linked polymer beads, where the fluorophore is covalently incorporated in the polymer backbone, thereby avoiding fluorophore leakage.

(b) These polymer beads are strongly emitting in the solid state also and have tunable emission colors.

(c) The tunability of the emission colors with more than one color from the same polymer particle makes it very convenient to use for labeling studies where one can access different emission regions just by exciting at the appropriate wavelength without having to label with different fluorophores.

(d) The versatility of the method allows for extending the approach to other commercially important polymers like PMMA also.

MATERIALS

Perylene-3,4,9,10-tetracarboxylic dianhydride (PTCDA), 3-pentadecyl phenol, zinc acetate, imidazole, poly (vinylpyrrolidone) (PVP, M_w 360,000 g/mol), acrylic acid, 4-methoxyphenol, 2-ethylhexylbromide, triethylphosphite, 4-hydroxy benzaldehyde, and potassium-tert-butoxide were purchased from Aldrich and used without further purifications. Styrene (Aldrich) was washed with sodium hydroxide followed by water, dried overnight using calcium chloride, and vacuum distilled before use. HBr in glacial acetic acid, para-formaldehyde, potassium carbonate, potassium iodide, dimethyl sulfoxide, dimethylformamide (DMF), tetrahydrofuran (THF), dichloromethane (DCM), and 2-chloroethanol were purchased locally and purified using standard procedures. Triton X-100 (70% solution in water) and 2,2′-azobis-(isobutyronitrile) (AIBN) were purchased from Merck and the latter was recrystalised from Methanol.

Measurements. ^{13}C and ^{1}H NMR spectra were recorded in $CDCl_3$ using Bruker AVENS 400 MHz spectrophotometer for small molecules (**PBI-PDP-TEG Diol, PBIX**, and **OPVX**), while the polymer samples were recorded using Bruker AVENS 500 MHz spectrophotometer. Chemical shifts (δ) are reported in ppm at 298 K, with trace amount of tetramethylsilane (TMS) as internal standard. MALDI-TOF analysis was carried out on a Voyager-De-STRMALDI-TOF (Applied Biosystems, Framingham, MA, USA) instrument equipped with 337 nm pulsed nitrogen laser used for desorption and ionization. The mode of operation was in a reflector mode with an accelerating voltage of 25 kV. Micromolar solutions of the compounds in THF were mixed with Dithranol matrix and spotted on stainless steel MALDI plate and dried well. Size exclusion chromatography (SEC) in chloroform was done using polystyrene standards for calibration using a polymer lab PL-220 GPC instrument. The flow rate of the chloroform was maintained as 1 mL throughout the experiments, and 2−3 mg in 1 mL of the samples were filtered and injected for recording the chromatograms at 30 °C. Thermogravimetric analysis (TGA) was performed using a PerkinElmer STA 6000 thermogravimetric analyzer. Samples were run from 40 to 800 °C with a heating rate of 10 °C/min under nitrogen. Absorption spectra were recorded using Perkin-Elmer Lambda 35 UV-spectrophotometer. Steady-state fluorescence studies were performed using Horiba Jobin Yvon Fluorolog 3 spectrophotometer having a 450 W xenon lamp. The emission and excitation slit width was maintained at 1 nm throughout the experiments, and the data was obtained in "S1/R1" mode (to account for the variations in lamp intensity). The solid state quantum yield was measured using a Model F-3029, Quanta-Phi 6″ Integrating Sphere connected with a Horiba Jobin Yvon Fluorolog 3 spectrophotometer. FEI, QUANTA 200 3D Scanning Electron Microscope with tungsten filament as electron source was used for recording SEM images. One mg of polymer dispersed in 2 mL of ethanol was drop cast on silicon wafers, and the solvent was allowed to evaporate at room temperature in air for 12 h. Before recording the morphology, films were coated by 5 nm thick gold film by sputtering method. Transmission Electron microscopy (TEM) was done using an FEI-Tecnai-F20 electron microscope operating at 200 kV. 0.5 mg of polymer dispersed in 2 mL of ethanol was deposited directly on carbon coated copper grid, and the solvent was allowed to evaporate at room temperature in air for 12 h. DLS measurements were carried out on Zetasizer ZS 90 apparatus, utilizing 633 nm red laser (at 90° angle) from Malvern instruments. The reproducibility of the data was checked at least three times using freshly prepared independent polymer solutions. The fluorescence microscopic images were taken by Epi-fluorescence microscope Leitz Labor Lux, Germany, and images were observed by a cannon power shot S-80 camera (excitation wavelength: 488−520 nm, green filter for OPV, and 550−550 nm, red filter for PBI). For sample preparation, very dilute dispersion of polymers in ethanol was drop cast onto a glass plate, covered with a coverslip, and directly observed under fluorescence microscope.

Scheme 1. Synthesis of Perylenebisimide Based Cross-Linker (PBIX)[a]

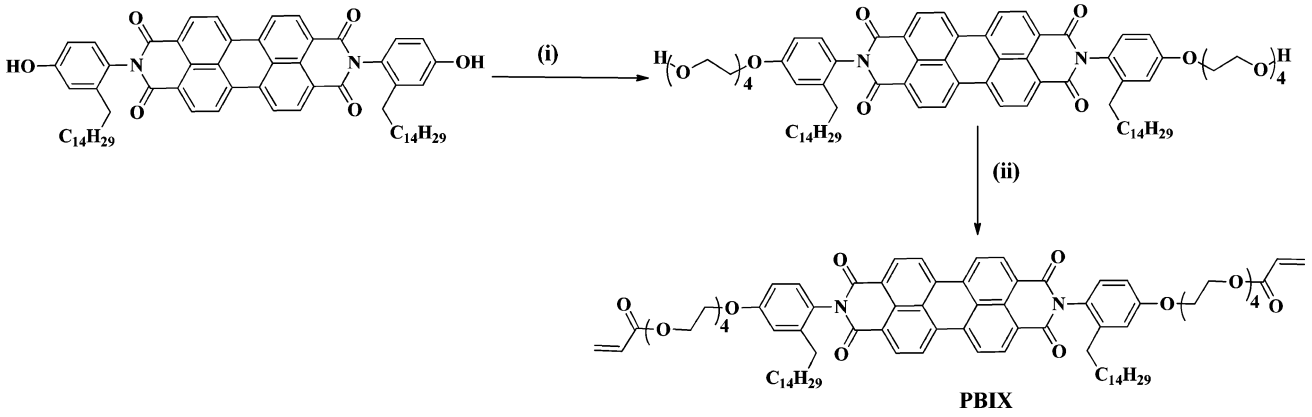

[a]Reagents: (i) TEG-monotosylate, K_2CO_3, DMF, 0−25−90 °C, 48 h, N_2. (ii) Acryloyl chloride, DCM, Et_3N, 0−25 °C, 24 h, N_2.

Scheme 2. Synthesis of Oligo(*p*-phenylenevinylene) Based Cross-Linker (OPVX)[a]

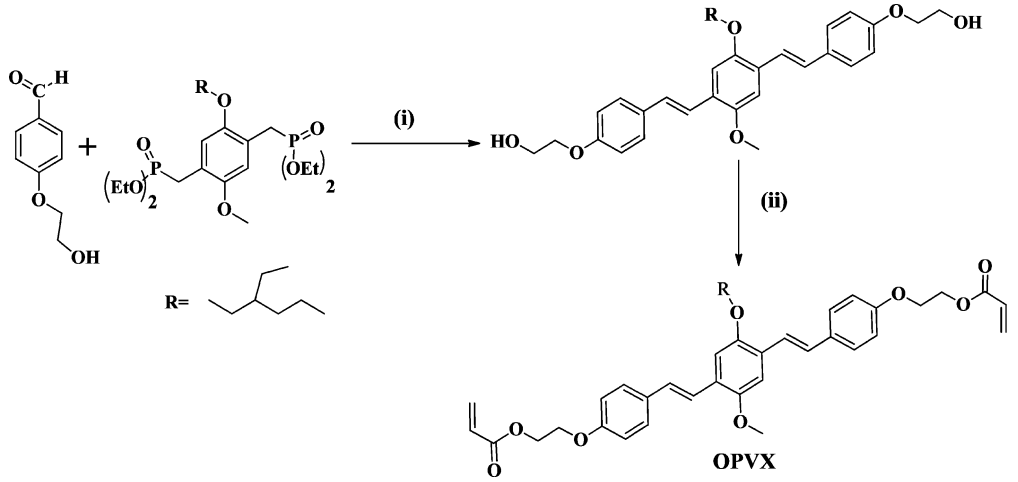

[a]Reagents (i) K-t-OBu, THF, 0−25 °C, 24 h. (ii) Acryloyl chloride, DCM, Et_3N, 25 °C, 24 h, N_2.

Synthesis of PBI-PDP-TEG Diol. The synthesis of the symmetric PDP substituted perylene bisimide derivative (PBI-PDP-diol) is reported in our earlier publication.[33] In a two necked round-bottom flask attached with reflux condenser, 3.5 g (0.0035 mol) of PBI-PDP-Diol, KI (0.02 g), and 4.88 g (0.035 mol) of K_2CO_3 were taken along with 150 mL of dry DMF under N_2 atmosphere. The reaction mixture was refluxed for one hour and then brought to room temperature (25 °C). 2.8 g (0.008 mol) of TEG-monotosylate in DMF was added over a period of thirty minutes at 0 °C to the above reaction mixture. The reaction mixture was stirred for 1.5 h at 0−5 °C, following which it was refluxed for 48 h at 85−90 °C. The reaction was monitored by TLC. For workup, the reaction mixture was cooled to 25 °C and poured into 20% HCl solution. The precipitate was filtered, washed with water, and dried under vacuum at 75 °C for 12 h. The compound was purified by column chromatography in DCM/methanol (5%) as solvent. Yield = 3.7 g (58%). ^{1}H NMR (200 MHz, CDCl3, δ ppm): 8.8−8.7 (m, 8H, Perylene ring), 7.13 (dd, 2H, Ar-PDP), 6.96 (m, 4H, Ar-PDP), 4.55 (t, 4H, Ar-OC**H**$_2$), 4.21 (t, 4H, Ar-OC**H**$_2$), 3.92−3.75 (bm, 24H), 2.37 (t, 4H), 1.51 (m, 4H), 1.08−1.19 (m, 48H, alkyl chain), 0.84 (t, 6H). MALDI-TOF MS (Dithranol matrix): *m*/*z* calcd for $C_{82}H_{110}N_2O_{14}$: 1346.80; found 1346.60 + 23 [M+Na$^+$] 1346.60 [M+K$^+$].

Synthesis of PBIX. In a 250 mL two necked round-bottom flask, 1.00 g (0.00075 mol) of PBI-PDP-TEG diol, 0.4 mL (0.0037 mol) of Et_3N, and dry DCM (80 mL) were taken under nitrogen atmosphere and stirred well at 0 °C for half hour. Acryloyl chloride 0.3 mL (0.0037 mol) in DCM was added to the reaction mixture over a period of 15−20 min at 0 °C. Reaction was carried out for 24 h at room temperature and monitored by TLC. For workup, the organic layer was washed with water and brine and extracted into DCM. The compound was purified by column chromatography in DCM/methanol (4%) as solvent. Yield = 0.7 g (70%). ^{1}H NMR (200 MHz, $CDCl_3$, δppm): 8.72 (m, 8H, Perylene ring), 7.11 (dd, 2H, Ar-PDP), 6.98 (m, 4H, Ar-PDP), 6.38 (dd, 2H, acrylic double bond), 6.17 (q, 2H, acrylic double bond), 5.85 (dd, 2H, acrylic double bond), 4.33 (t, 4H, Ar-OC**H**$_2$), 4.20 (t, 4H, Ar-OC**H**$_2$), 3.89−3.74 (bm, 24H), 2.4 (t, 4H), 1.51 (m, 4H), 1.08−1.19 (m, 48H, alkyl chain), 0.84 (t, 6H). ^{13}C NMR (400 MHz, $CDCl_3$)166.1, 163.58, 159.1, 141.5, 134.8, 131.8, 131.0, 129.6, 128.2, 126.5, 123.4, 123.2, 116.0, 112.6, 70.8, 70.6, 69.1 67.4, 63.7, 31.8, 29.6, 29.5, 29.3, 27.2, 22.6, 14.1. MALDI-TOF MS (Dithranol matrix): *m*/*z* calcd for $C_{40}H_{42}N_2O_4$: 1456.8; found 1479 + 23 [M +Na$^+$], 1479 + 23 + 39 [M+Na$^+$ K$^+$], 1478 + 39 + 39 [M+2K$^+$].

Synthesis of OPV Cross-Linker. The symmetric OPV diol was synthesized as reported in the literature.[34] In a 250 mL two necked round-bottom flask, 1.1 g (0.00196 mol) of OPV Diol was taken along with 1 mL (0.01 mol) of Et_3N, and dry DCM (80 mL) under nitrogen atmosphere and stirred well at 0 °C for half an hour. Acryloyl chloride (0.64 mL, 0.0078 mol) in DCM was added to the reaction mixture for a period of 15−20 min at 0 °C. The reaction was carried out for 24 h at room temperature and monitored by TLC. For workup, the organic layer was evaporated, and the compound was purified by column chromatography in 20% ethyl acetate/pet ether solvent combination. Yield = 0.45 g (41%) ^{1}H NMR (200 MHz, $CDCl_3$, δppm): 7.46−6.92 (3m, 14H, Ar−H, and vinylic H), 6.41 (dd, 2H, acrylic double bond), 6.18 (m, 2H, acrylic double bond), 5.89 (dd, 2H, acrylic double bond),

Table 1. Sample Designation, Number and Weight Average Molar Mass, Polydispersity Indices (PDI), Yield, and 5 Wt % Loss Temperature of the PS/PBI/OPV Based Polymers

sr no.	sample name	moles in feed	moles of cross-linker incorporation from UV[a]	yield (%)	M_n[b]	M_W[b]	PDI	TGA[c] (T_d = 5%)
1	**PS-PBI-0.16**	3.4×10^{-6}	1.6×10^{-7}	80	40,000	99,900	2.5	345
2	**PS-PBI-1.0**	6.8×10^{-6}	1×10^{-6}	78	24,800	91,600	3.7	345
3	**PS-PBI-2.7**	1×10^{-5}	2.7×10^{-6}	76	37,900	154,000	4.0	345
4	**PS-PBI-3.8**	1.4×10^{-5}	3.8×10^{-6}	75	32,400	149,000	4.6	345
5	**PS-OPV-0.38**	3.7×10^{-6}	3.8×10^{-7}	80	24,900	99,000	4	340
6	**PS-OPV-1.8**	7.5×10^{-6}	1.8×10^{-6}	82	34,700	18,0000	5.1	340
7	**PS-OPV-2.9**	1.5×10^{-5}	2.9×10^{-6}	86	17,600	670,000	4.4	340
8	**PS-OPV-5.12**	2.2×10^{-5}	5.12×10^{-6}	85	19,400	63,000	3.5	340
9	**PS-PBI-0.82-OPV-0.88**	3.4×10^{-6} 3.7×10^{-6}	8.2×10^{-7} 8.8×10^{-7}	80	21,000	78,300	3.7	340
10	**PS**	-	-	90	40,200	1,24,800	3.10	320
11	**PS-DVB**	-	-	78 (insoluble)	-	-	-	340

[a]Measured in chloroform. [b]Measured by size exclusion chromatography (SEC) in chloroform ($CHCl_3$), calibrated with linear, narrow molecular weight distribution polystyrene standards. [c]TGA measurements at heating rate of 10 °C/min under nitrogen.

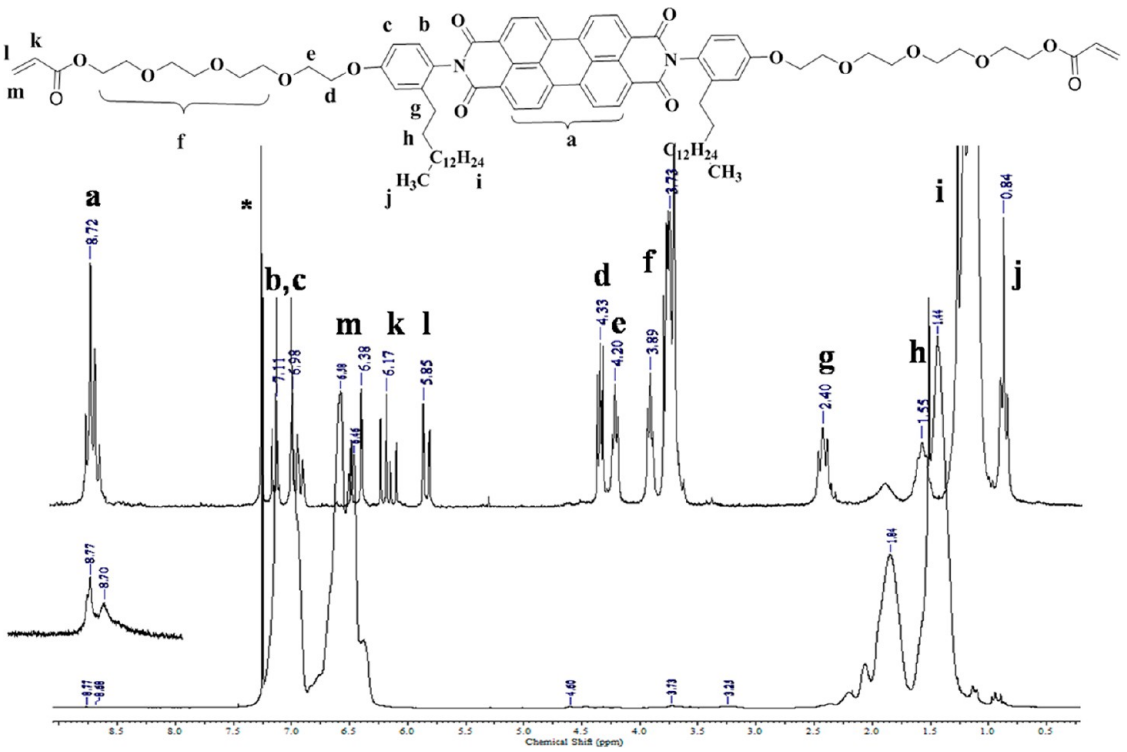

Figure 1. Comparison of the ^{1}H NMR spectra of **PS-PBI-3.8** polymer with **PBIX** recorded in $CDCl_3$.

4.52 (m, 2H, ArOC**H**$_2$), 4.23 (m, 2H, C(O)OC**H**$_2$), 3.90 (s, 3H, ArOC**H**$_3$) 3.90 (d, 2H, ArOC**H**$_2$), 1.70−1.37 (m, 9H, alkyl protons), 0.97−0.90 (t, 6H). ^{13}C NMR (400 MHz, $CDCl_3$)165.8, 157.7, 151.0, 150.9, 131.0, 127.8, 127.5, 127.4, 126.4, 121.2, 114.6, 109.9, 108.7, 71.5, 65.7, 62.6, 56.1, 39.5, 30.6, 29.0, 23.9, 22.8, 13 0.8, 11.0 MALDI-TOF MS (Dithranol matrix): *m*/*z* calcd for $C_{41}H_{48}O_8$: 668.8; found 668.5 [M^+]

Two Stage Dispersion Polymerization Procedure To Prepare PS-PBI/OPV-X. *Procedure.* The stabilizer (PVP), the costabilizer (Triton X-305), initiator (AIBN), and half of the styrene monomer and ethanol were added to a 250 mL three necked reaction flask equipped with a gas inlet, overhead stirrer, and rubber septum. After a homogeneous solution formed at room temperature, the solution was deoxygenated by bubbling nitrogen gas at room temperature for at least 30 min. Then the flask was placed in a 70 °C oil bath and stirred mechanically at 120 rpm. The cross-linker (**PBIX**/**OPVX**) was dissolved in the remaining styrene and ethanol at 60 °C under nitrogen. After the cross-linker had dissolved and the polymerization reaction had run for 1 h, the hot styrene-cross-linker solution was added into the reaction flask over a period of 3 h (drop by drop addition). The reaction was continued for 4 h under continuous flow of nitrogen with overhead stirring. The precipitated polymer in the reaction medium was washed with 200 mL × 4 times of methanol and separated by centrifuge. The polymer was dried under vacuum at 50 °C for 6 h. The polymerization recipe is given in Supporting Information Table S1.

RESULTS AND DISCUSSION

Synthesis and Characterization. The synthesis of the fluorescent cross-linkers based on perylenebisimide (**PBIX**) and oligo(*p*-phenylenevinylene) (**OPVX**) is shown in Schemes 1 and 2, respectively. **PBIX** was synthesized starting with the imidization of perylenetetracarboxylic anhydride with 4-amino-

3-pentadecyl phenol. The details of the synthesis to obtain the final acryloyl functionalized cross-linker is given in the experimental section. In a similar manner the hydroxyl functionalized OPV molecule was coupled with acryloyl chloride to obtain the **OPVX** cross-linker. The structure and purity of the cross-linkers were confirmed by ^{1}H NMR, MALDI, and also by the single peak in the SEC chromatogram (Supporting Information S2 to S6). The MALDI spectra of **PBIX** showed peaks at higher mass corresponding to single as well as multiple sodium and potassium adducts which could be attributed to the alkali metal ion coordination with the ethylene glycol segments on the **PBIX** backbone. The two-stage dispersion polymerization recipe to incorporate the fluorescent cross-linkers **PBIX** and **OPVX** into PS backbone is given in the Supporting Information (Table S1).Varying amounts of the cross-linker (5−20 mg; 3.4 to 14 μM) (0.13 to 0.51 wt % w.r.t. styrene) were taken in the feed to obtain a series of lightly cross-linked polystyrene. One cross-linked PS was synthesized using both **PBIX** and **OPVX** ∼ 3.0 × 10^{-6} mols each. The highest amount of the cross-linker that could be added in the feed during the second stage without the dispersion crashing out was 14 μM. The actual incorporation of the PBI as well as OPV based cross-linker into the PS backbone was determined using Beer−Lamberts Law using the molar extinction coefficient of the respective cross-linker (**PBIX** = 62082 L·M^{-1}·cm^{-1}, **OPVX** = 36315 L·M^{-1}·cm^{-1}).[35,36] The cross-linked PS with **PBIX** and **OPVX** were named as the **PS-PBI-X** and **PS-OPV-X** series respectively, where 'x' indicated the amount (in μM) of the respective cross-linker incorporated. Table 1 gives the fluorophore incorporation determined from UV−vis studies. The PS remained completely soluble for the highest cross-linker incorporation also (∼5 μM). The complete solubility of these lightly cross-linked polystyrene in common organic solvents enabled the structural characterization using proton NMR spectroscopy and UV−vis absorption spectroscopy as well as molecular weight determination using size exclusion chromatogram (SEC). The molecular weight of the cross-linked PS was determined by SEC using chloroform as the eluent. The GPC chromatogram is given in the Supporting Information Figure S7. Higher incorporation of the rigid cross-linker resulted in considerable reduction in the M_w values especially in the case of **PS-OPV-X** polymers. Table 1 gives the molecular weight determined by SEC along with that of PS alone prepared under identical conditions. Cross-linking is known to improve the thermal stability of the polymers;[37] the **PS-PBI/OPV-X** series of cross-linked polymers had higher thermal stability compared to uncross-linked PS as determined by the thermogravimetric analysis. PS had a 5 wt % loss at 320 °C, while the **PS-PBI/OPV-X** cross-linked polymers exhibited 5 wt % loss at a much higher temperature of 340−345 °C. A 3 mol % divinylbenzene (DVB) cross-linked PS prepared by the two stage dispersion polymerization under identical conditions also exhibited a 5 wt % loss temperature of 340 °C. Table 1 lists the 5 wt % loss temperature, and Supporting Information Figure S8 gives the TGA plot. Figure 1 shows the labeled proton NMR spectra of the perylenebisimide cross-linker **PBIX** along with the cross-linked polystyrene with 3.8 μM PBI incorporation **PS-PBI-3.8**. The eight aromatic protons of the perylene ring at 8.72 ppm matched very well in intensity with the six protons of the acrylic double bond in the region 5.8 to 6.48 ppm for **PBIX**. The inset in the top spectra shows the perylene aromatic protons which had become broad after incorporation in the polystyrene. The aromatic protons of the PDP ring were merged with the aromatic peaks of PS. In the case of the **PS-OPV-X**, the aromatic protons of the OPV were completely overlapped by the aromatic protons of PS thereby making it difficult to observe the peaks corresponding to the **OPVX** in the cross-linked polymer. The proton NMR spectra of **PS-PBI-0.82-OPV-0.88** having both perylenebisimide and oligo(*p*-phenylenevinylene) incorporation is given in Supporting Information Figure S9.

Microscopic Characterization. The dispersity of the cross-linked PS particles was determined using dynamic light scattering (DLS) studies carried out in ethanol dispersion. The samples showed an average particle size of 2−3 μm with increasing size for higher cross-linker incorporation. Figure 2

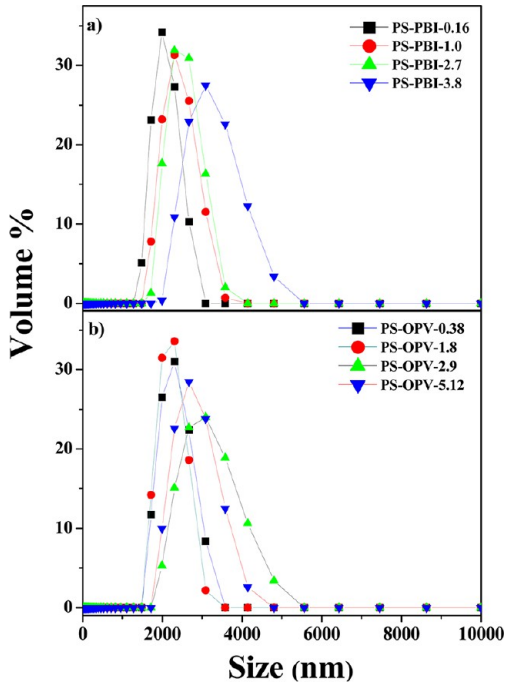

Figure 2. Volume − average size distribution of (a) **PS-PBI-X** and (b) **PS-OPV-X** series in ethanol dispersion obtained by dynamic light scattering (DLS) analysis.

shows the DLS curves for **PS-PBI-X** and **PS-OPV-X** series which clearly indicated narrower particle size distribution for low incorporation of cross-linker. The SEM images also supported the narrow particle size distribution. Figure 3 shows the SEM and TEM images for **PS-PBI-0.16**. In both cases the spherical particles were nearly monodisperse with an average diameter of 2.0 μm. Similarly, Figure 4 shows the SEM and TEM images for **PS-OPV-0.38** showing the almost monodisperse nature of particle with average size ∼2.6 μm. Fluorescence microscope images of ethanol dispersion of samples drop cast on glass substrate demonstrated the emission from the fluorescent cross-linked PS. Figure 5 (top) images show the emission of **PS-PBI-0.16** beads, while the (bottom) images correspond to those for **PS-OPV-0.38**. The average particle size observed from the fluorescence images were ∼1.7 μm for **PS-PBI-0.16** and ∼1.4 μm for **PS-OPV-0.38**, respectively. This was in accordance with the sizes observed from SEM and TEM images of the samples indicating their nearly monodisperse nature. Supporting Information Figure S10 shows the fluorescence microscope image of the **PS-PBI-X** and **PS-OPV-X** series, respectively. Figure 6 shows the SEM

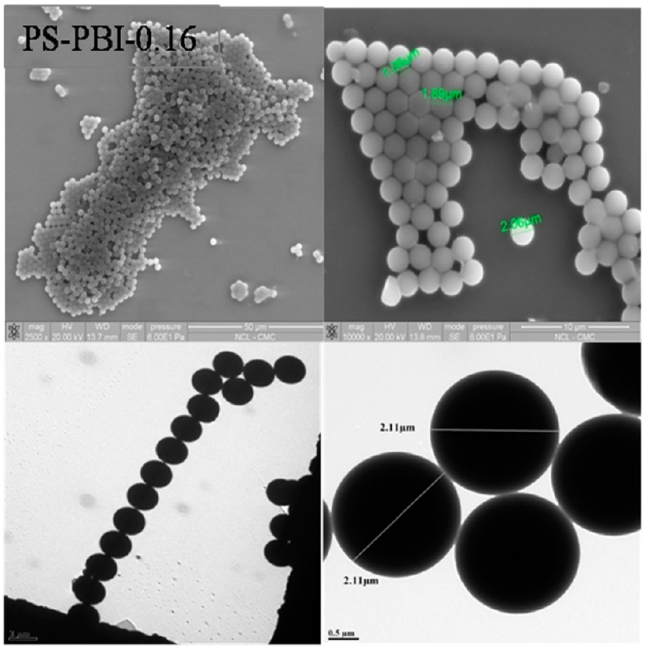

Figure 3. (top) SEM images of **PS-PBI-0.16** drop cast on silicon wafer (1 mg/2 mL ethanol dispersion) and (bottom) TEM images (0.5 mg/2 mL ethanol dispersion) drop cast on carbon coated copper grids.

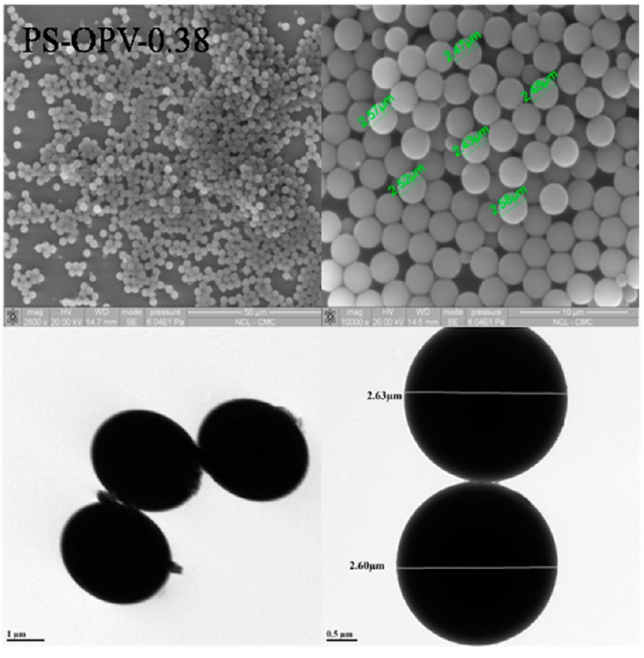

Figure 4. (top) SEM images of **PS-OPV-0.38** drop cast on silicon wafer (1 mg/2 mL ethanol dispersion) and (bottom) TEM images (0.5 mg/2 mL ethanol dispersion) drop cast on carbon coated copper grids.

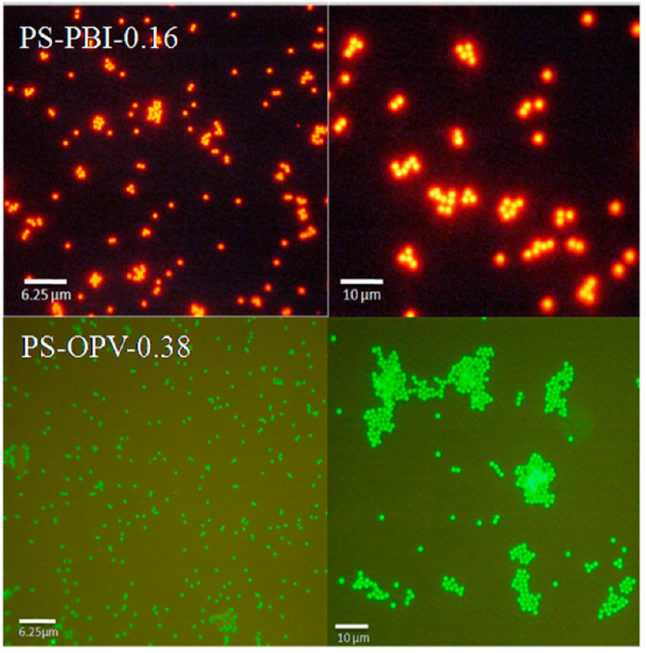

Figure 5. Fluorescence optical microscopy images of **PS-PBI-0.16** using 500−550 nm, red filter (top) and **PS-OPV-0.38** is using 488−520 nm, green filter (bottom).

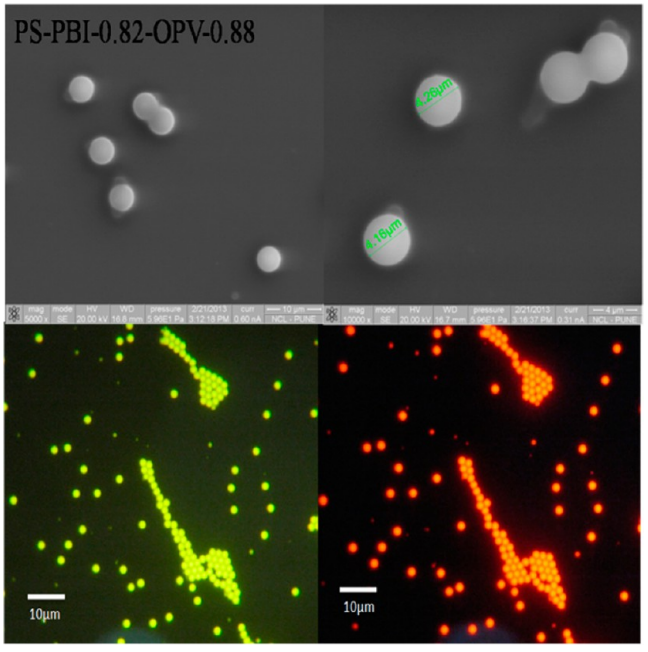

Figure 6. (top) SEM images of **PS-PBI-0.82-OPV-0.88** drop cast on silicon wafer (1 mg/2 mL ethanol dispersion) and (bottom) fluorescence optical microscopy images using 500−550 nm, red filter for PBI and using 488−520 nm, green filter for OPV imaging.

(top) and fluorescence microscope images (bottom) for the **PS-PBI-0.82-OPV-0.88** sample. The particle size obtained from SEM images was slightly higher (∼4 μm) than that of the cross-linked PS particles incorporating either PBI or OPV alone. However, the fluorescence microscope image indicated an average particle size of 2.5 μm, whereas DLS data of the ethanol dispersion of **PS-PBI-0.82-OPV-0.88** showed a much smaller particle size ∼1.5 μm as given in Supporting Information Figure S11. The dual emission from the sample was clearly observable from the fluorescence images (Figure 6 bottom) upon using the green and red filter for OPV and PBI emission, respectively. The green filter (transparent in the range 488−520 nm) allowed for some of the PBI emission also to filter through, resulting in the yellow-green emission of the particles in contrast to the green emission from the **PS-OPV-0.38** sample.

Photophysical Characterization. The photophysical characteristics of the fluorescent cross-linked PS beads were

determined by recording the absorption and emission spectra of 0.1 OD (at the absorption wavelength maxima) solution in chloroform. Figure 7 compares the normalized (at peak

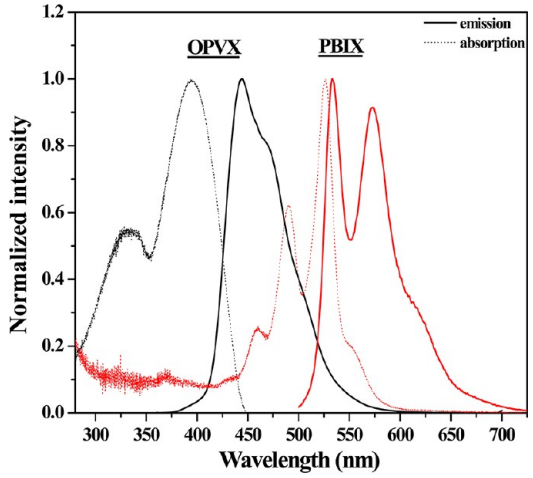

Figure 7. Normalized absorption and Emission spectra of **PBIX** and **OPVX** in (0.1 OD at 370 nm; λ_{ex} = 370 nm for **OPVX** and 0.1 OD at 527 nm; λ_{ex} = 490 nm for **PBIX**).

maxima) absorption and emission spectra of the cross-linkers **PBIX** and **OPVX**, respectively. The absorption spectra of **PBIX** exhibited peaks in the range of 400−530 nm, corresponding to the S_0-S_1 transition with well resolved vibronic structure from 0−0, 0−1, 0−2, and 0−3 transitions, respectively. The emission spectrum had emission wavelength maxima at 535 nm. The **OPVX** had absorption maxima at 390 nm and emission wavelength maxima at 430 nm. The fluorescence quantum yields of the two cross-linkers were determined by the relative method using rhodamine-6G in ethanol as a standard for PBI (λ_{ex}: 490 nm) and quinine sulfate solution in 0.5 M H_2SO_4 solution as the standard for OPV (λ_{ex}: 370 nm) (see Table 2).

Table 2. Photoluminescence Quantum Yield Measured As Powder and in $CHCl_3$ Solution

		$CHCl_3$		powder	
sr no.	polymer	λ_{ex} (nm)	ϕ	λ_{ex} (nm)	ϕ
1	**PBIX**	490	0.27	490	0.055
2	**OPVX**	350	0.88	350	0.037
3	**PS-PBI-0.16**	490	0.33	490	0.25
4	**PS-OPV-0.38**	350	0.66	350	0.71
5	**PS-PBI-0.82-OPV-0.88**	490	0.34	490	0.33 (PBI)
		350	0.57	350	0.20 (OPV)

The values were ϕ_{PBI} = 0.27 and ϕ_{OPV} = 0.88 for **PBIX** and **OPVX**, respectively. The absorption and emission spectra were recorded for the **PS-PBI-X** and **PS-OPV-X** series in chloroform. Figure 8a shows the absorption and emission (dotted line) spectra of **PS-OPV-0.38**; the corresponding spectra for **OPVX** is also given for the sake of comparison. Upon incorporation in the PS backbone a blue shift of ∼40 nm was observed in the absorption spectra of **PS-OPV-2.5** (390 nm for **OPVX** to 350 nm for **PS-OPV-0.38**). A similar blue shift of 37 nm was observed in the emission spectra of the polymer also, and the emission had two peaks at 407 and 413 nm. A probable reason for this blue shift is the stacking of the aromatic units of

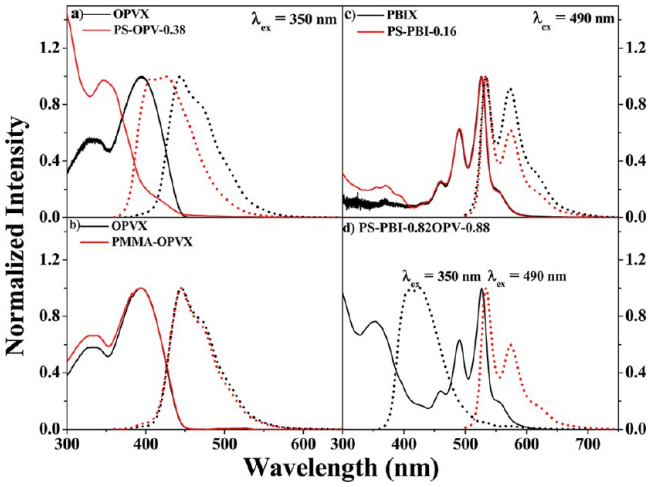

Figure 8. Absorption (solid line) and emission spectra (dotted line) of (a) **OPVX** (0.1 OD at 370 nm; λ_{ex} = 350 nm) and **PS-OPV-0.38** (0.1 OD at 350 nm, λ_{ex} = 350 nm), (b) **OPVX** (0.1 OD at 370 nm; λ_{ex} = 350 nm) and PMMA-OPVX, and (c) **PBIX, PS-PBI-0.16** (0.1 OD at 527 nm; λ_{ex} = 490 nm) along with (d) **PS-PBI-0.82-OPV-0.88** (0.1 OD at 350 nm, λ_{ex} = 350 nm and 0.1 OD at 527 nm; λ_{ex} = 490 nm) in $CHCl_3$.

PS surrounding the OPV chromophores. To investigate this, the **OPVX** was incorporated into PMMA backbone by a two stage dispersion polymerization route. Figure 8b compares the absorption and emission spectra of **PMMA-OPVX** along with **OPVX** recorded in chloroform. The **PMMA-OPVX** did not exhibit any shift in absorption or emission and was exactly identical to that of the **OPVX**, validating the reasoning that the blue shift observed in the case of the **PS-OPV-X** was due to the presence of the aromatic PS units enveloping the OPV chromophore. Figure 8c shows the absorption and emission (dotted line) spectra of **PS-PBI-0.16** along with that of the cross-linker **PBIX. PBIX** did not show any changes or shift in wavelength upon incorporation in the PS backbone and had similar absorption and emission wavelength maxima. Figure 8d shows the absorption and emission spectra of **PS-PBI-0.16-OPV-0.38**, which had both OPV and PBI incorporated. Its absorption spectra had contribution from both the chromophores with a broad OPV absorption in the 350 nm region and a vibrationally fine structured absorption corresponding to PBI in the range 400−530 nm. Upon excitation at the perylene absorption of 490 nm, emission corresponding to PBI was observed at 533 nm. Upon excitation at the OPV wavelength of 350 nm, intense emission corresponding to OPV with peak maxima at 407 and 413 nm were observed along with small emission corresponding to PBI. A possible energy transfer from OPV to PBI was ruled out since PBI also has absorption in the range ∼350 nm making selective excitation of OPV impossible. In fact, excitation of the PBI alone polymer − **PS-PBI-0.16** (0.1 OD at 350 nm) at 350 nm also showed emission similar in intensity to that of the **PS-PBI-0.82-OPV-0.88** indicating that the observed emission from perylene upon excitation at the OPV wavelength could probably be due to direct excitation of PBI.

The highlight of the present work was the solid state monomeric (nonagregated) emission from the cross-linked monodispersed, thermally stable PS beads. The very pale pink colored **PS-PBI-X** and colorless **PS-OPV-X** samples upon observation under hand-held UV lamp emitted intense orange

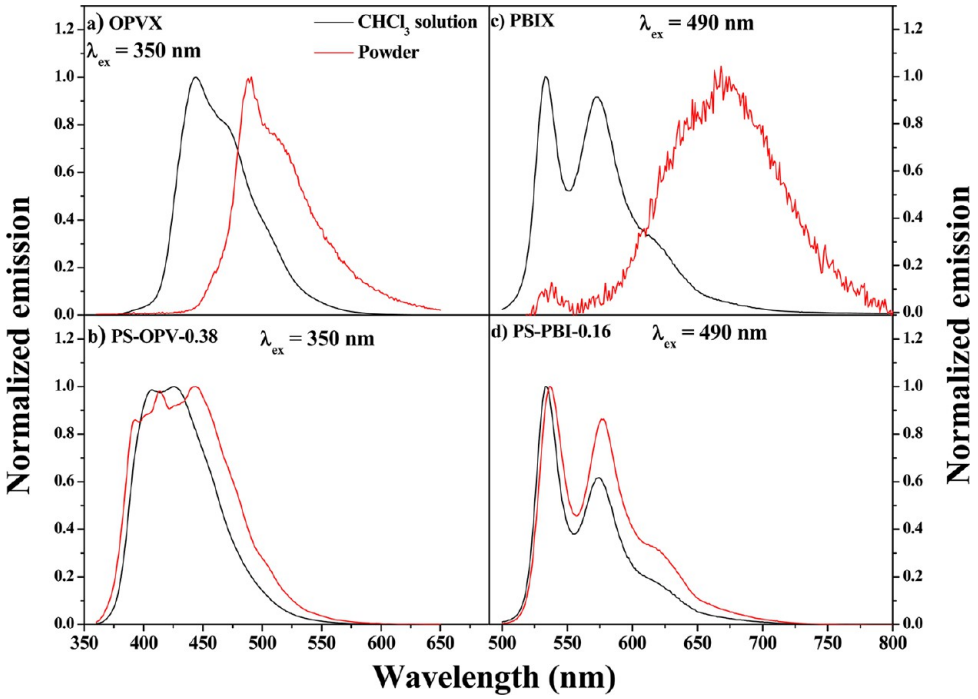

Figure 9. Comparison of the emission spectra in the solution state in chloroform and solid state for the cross-linkers and polymer. a) **OPVX** in $CHCl_3$ and as powder upon excitation at 350 nm, (b) **PS-OPV-0.38** in $CHCl_3$ and as powder upon excitation at 350 nm, (c) **PBIX** in $CHCl_3$ and as powder upon excitation at 490 nm, and (d) **PS-PBI-0.16** in $CHCl_3$ and as powder upon excitation at 490 nm.

and blue fluorescence, respectively. Supporting Informaiton Figure S12 shows the images of the powdered PS samples both under normal and UV light. Supporting Information Figure S13 compares the solid state absorption spectra (recorded in the reflectance mode) of the **PS-PBI-0.16, PS-OPV-0.38**, and **PS-PBI-0.82-OPV-0.88** powders. The absorption corresponding to the OPV was so weak that it was not observable in the powder state. The PBI chromophore has a higher molar absorption coefficient compared to OPV chromophore; therefore, peaks corresponding to the perylene absorption were visible in the solid powder form. Comparing the absorption spectra of **PS-PBI-0.16** recorded as a solid powder with that in chloroform, the (0,1) vibronic transition had higher intensity in the former compared to the latter (Supporting Information Figure S14). However no red shifting of the absorption maxima characteristic of aggregation was observed in the solid state absorption spectra.

Figure 9 compares the normalized emission spectra of the cross-linkers and polymers recorded in the powder form with the corresponding spectra recorded in chloroform solution. The cross-linkers exhibited very weak emission in the solid state. Figure 9a compares the spectra for the cross-linker **OPVX** upon excitation at 350 nm. The spectra in the solid state was red-shifted by 46 nm (peak maxima at 490 nm) compared to that in solution indicating aggregation in the solid state. Figure 9b compares the emission spectra of **PS-OPV-0.38** recorded in powder form and in solution. In contrast to the red shift observed for the cross-linker, no red shift was observed for the emission of **PS-OPV-0.38** in the solid compared to that in solution. The emission in the solid state had a maxima centered ~400 nm with vibrational fine structure. The vibronic structure indicated the absence of pronounced molecular interactions among the OPV chromophores distributed in the PS backbone in the solid state. As observed in the solution state, a blue shift of 45 nm was observed in the solid state emission spectra of the **PS-OPV-0.38** compared to **OPVX**. Figure 9c compares the solid and solution state emission spectra for **PBIX**. The solid state emission from **PBIX** was characterized by red-shifted emission from aggregates ~660 nm, which was absent in the solution state of the same sample. In the case of the cross-linked PS containing PBI i.e. **PS-PBI-0.16** (Figure 9d), the emission in the solid state was characterized by the higher intensity of the (0,1) vibrational transition compared to the (0,0) transition and a complete absence of aggregate emission >600 nm. The solid state fluorescence quantum yield ϕ_{powder} was determined using an integrating-sphere Quanta ϕ Horiba attachment under excitation at 490 nm for PBI and 350 nm for OPV, respectively. **PBIX** had low solid state quantum yield ϕ_{powder} of ~0.055; whereas **PS-PBI-0.16** had a high quantum yield ϕ_{powder} of ~0.25. The ϕ_{powder} of **OPVX** was very low ~0.037 compared to that of **PS-OPV-0.38**, which had a ϕ_{powder} ~ 0.71. Supporting Information Figure S15 compares the emission spectra of the cross-linked PS series of polymers in the powder form. The cross-linked PS with higher incorporation of OPV; namely **PS-OPV-1.8, PS-OPV-2.9**, and **PS-OPV-5.12** exhibited fluorescence with the PL intensity increasing with gradual red shift of peak maxima. In the case of the cross-linked PS containing PBI, no aggregate emission beyond 600 nm was observed.

Figure 10 compares the emission spectra of the cross-linked PS bead containing both PBI and OPV, viz; **PS-PBI-0.82-OPV-0.88**. It exhibited reduced emission intensity for OPV upon excitation at the OPV absorption wavelength maxima of 350 nm. Emission from the PBI in the range >500 nm was also observed upon excitation at 350 nm. Since molecular interactions among the chromophores were expected to be absent or negligibly low in the solid state, energy transfer from the OPV to PBI chromophore was not expected. Figure 10 also shows the emission from the PBI alone polymer i.e. **PS-PBI-0.16** upon excitation at 350 nm. **PBIX** had reasonable

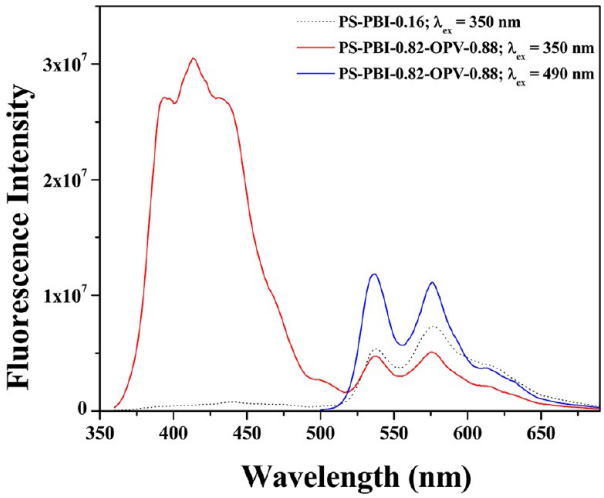

Figure 10. Solid state emission spectra of **PS-PBI-0.0.82-OPV-0.88** upon excitation at 350 and 490 nm. The emission from **PS-PBI-0.16** upon excitation at 350 nm is also given for comparison (dotted line).

absorption at 350 nm resulting in direct excitation of perylene upon excitation at 350 nm suggesting that selective excitation of **OPV** was not possible in the **PS-PBI-0.82-OPV-0.88** polymer. Excitation at 490 nm resulted in strong emission from PBI in the case of **PS-PBI-0.82-OPV-0.88**. The quantum yield for the **PBI** emission in **PS-PBI-0.82-OPV-0.88** was quite high at 0.33 compared to that for **OPV** which was 0.20.

PBI as well as **OPV** are chromophores well-known for their tendency to aggregate and lead to quenching of fluorescence in concentrated solution and solid state.[38−40] Sometimes strategies like introduction of bulky substitutes that can reduce aggregation induced fluorescence quenching or positive effects of aggregate emission based on some J-type aggregates have been reported in the literature especially for perylenebisimides to exhibit fluorescence in the solid state.[41−44] Some bay substituted perylene bisimides have been shown to exhibit intense fluorescence emission in the solid state.[45,46] The solid state emissions in most of these cases are aggregate emission in the ∼600 nm range.[47,48] Our current report is one of the few reports where these highly emitting fluorophores have been successfully incorporated into a polymer scaffold in the form of cross-linker and achieved fluorescent polymer beads with intense emission from the nonaggregated chromophore in the solid state.[19,42,49,50] The absolute quantum yield of the powder sample determined using the integrating sphere set up and the fluorescence microscopic images was proof for this. The fact that this approach allows the incorporation of simultaneous addition of multiple fluorophores emitting in different colors makes it very convenient to use for labeling studies where one can access different emission regions just by exciting at the appropriate wavelength without having to label with different fluorophores.

CONCLUSION

A series of cross-linked polystyrene microbeads incorporating fluorophores like perylene bisimide (**PBI**) and oligo(*p*-phenylenevinylene) (**OPV**) as the cross-linker were successfully developed by two stage dispersion polymerization strategy. Dispersion polymerization was adopted as the method of choice since it was more tolerant to rigid aromatic molecules with poor solubility and allowed their incorporation into the polymer backbone and still maintained control over the particle size distribution. The advantage of adapting the fluorophore itself as the cross-linker was 2-fold. One, fluorescent cross-linked polymer particles could be obtained in one shot without having to add two ingredients − the fluorophore and the cross-linker separately in the reaction medium and the covalent attachment of the dye to the polymer backbone avoided dye leakage. The second and most appealing reason was the ability of maximum emission from very low fluorophore incorporation as larger incorporation of fluorophores like PBI and OPV are known to result in aggregation induced quenching. Thus, using this strategy up to $\sim 5 \times 10^{-6}$ moles of the rigid fluorophores could be incorporated into PS backbone. The fluorescent spherical cross-linked PS beads had an average diameter of 2−3 μm. The PS beads incorporating PBI exhibited intense orange red emission in the solid state with quantum yield ϕ_{Powder} = 0.25, while the PS incorporating OPV as the cross-linker fluorophore exhibited intense green emission very high quantum yield of ϕ_{Powder} = 0.71. This is the first time that successful monomer emission (no emission from aggregate) with high quantum efficiency has been achieved from fluorophores based on **PBI** and **OPV**, which are known to undergo $\pi-\pi$ stacking interaction of their aromatic core in the solid state and even in highly concentrated form in solution resulting in quenching of their emission. An added advantage of this strategy of fluorophore as cross-linker was the ability to incorporate more than one tailor-made fluorophore into the PS backbone enabling fine-tuning of the emission colors. Fluorescent microbeads with stable intense emission find application in various areas, and the approach introduced here is expected to be a viable route toward their easy and reproducible development.

ASSOCIATED CONTENT

Supporting Information

Details of structural characterization of the monomers and polymers. This material is available free of charge via the Internet at http://pubs.acs.org.

AUTHOR INFORMATION

Corresponding Author

*E-mail: sk.asha@ncl.res.in.

Notes

The authors declare no competing financial interest.

ACKNOWLEDGMENTS

This work has been financially supported by the network project NWP0054. The authors thank Mr. Ketan Bhotkar, Mr. Pankaj Shankhpalli, and Mr. Ejaj Pathan, NCL − Pune for SEM, TEM imaging, and for the fluorescence microscope facility, respectively. We thank IISER-Pune for the DLS measurements. Swapnil thanks CSIR-New Delhi, India for Senior Research Fellowship. The authors also sincerely thank Dr. S. Sivaram (CSIR Bhatnagar Fellow, CSIR-NCL) for valuable suggestions and discussion.

REFERENCES

(1) Peng, B.; Wee, E.; Imhof, A.; Blaaderen, A. *Langmuir* **2012**, *28*, 6776−6785.
(2) Han, M.; Gao, X.; Su, J. Z.; Nie, S. *Nat. Biotechnol.* **2001**, *19*, 631−635.
(3) Diacon, A.; Rusen, E.; Mocanu, A.; Hudhomme, P.; Cincu, C. *Langmuir* **2011**, *27*, 7464−7470.

(4) Wu, S.-K.; Tang, T.-P.; Tseng, W. J. *J. Mater. Sci.* **2008**, *43*, 6453−6458.
(5) Tung, Y. C.; Zhang, M.; Lin, C. T.; Kurabayashi, K.; Skerlos, S. J. *Sens. Actuators, B* **2004**, *98*, 356−367.
(6) Sanchez-Martin, R. M.; Alexander, L.; Muzerelle, M.; Cardenas-Maestre, J. M.; Tsakiridis, A.; Brickman, J. M.; Bradley, M. *ChemBioChem.* **2009**, *10*, 1453−1456.
(7) Sukhanova, A.; Nabiev, I. *Crit. Rev. Oncol./Hematol.* **2008**, *68*, 39−59.
(8) Holzapfel, V.; Musyanovych, A.; Landfester, K.; Lorenz, M. R.; Mailander, V. *Macromol. Chem. Phys.* **2005**, *206*, 2440−2449.
(9) Medintz, I. L.; Uyeda, H. T.; Goldman, E. R.; Mattoussi, H. *Nat. Mater.* **2005**, *4*, 435−446.
(10) Chan, Y.; Zimmer, J. P.; Stroh, M.; Steckel, J. S.; Jain, R. K.; Bawendi, M. G. *Adv. Mater.* **2004**, *16*, 2092−2097.
(11) Martín-Banderas, L.; Rodríguez-Gil, A.; Cebolla, Á.; Chávez, S.; Berdún-Álvarez, T.; Garcia, J. M. F.; Flores-Mosquera, M.; Gañán-Calvo, A. M. *Adv. Mater.* **2006**, *18*, 559−564.
(12) Ribeiro, T.; Baleizão, C.; Farinha, J. P. S. *J. Phys. Chem. C* **2009**, *113*, 18082−18090.
(13) Yang, Z.; Wang, Z.; Yao, X.; Wang, Y. *Langmuir* **2012**, *28*, 3011−3017.
(14) Sadovoy, A. V.; Lomova, M. V.; Antipina, M. N.; Braun, N. A.; Sukhorukov, G. B.; Kiryukhin, M. V. *ACS Appl. Mater. Interfaces* **2013**, *5*, 8948−8954.
(15) Jung, Y.; Hickey, R. J.; Park, S. J. *Langmuir* **2010**, *26*, 7540−43.
(16) Yabu, H.; Tajima, A.; Higuchic, T.; Shimomura, M. *Chem. Commun.* **2008**, 4588−4589.
(17) Schütze, F.; Stempfle, B.; Jüngst, C.; Wöll, D.; Zumbusch, A.; Mecking, S. *Chem. Commun.* **2012**, 2104−2106.
(18) Dullens, R. P. A.; Claesson, E. M.; Kegel, W. K. *Langmuir* **2004**, *20*, 658−664.
(19) Baier, M. C.; Huber, J.; Mecking, S. *J. Am. Chem. Soc.* **2009**, *131*, 14267−14273.
(20) Tuncel, D.; Demir, H. V. *Nanoscale* **2010**, *2*, 484−494.
(21) Shelton, A. H.; Price, R. S.; Brokmann, L.; Dettlaff, B.; Schanze, K. S. *ACS Appl. Mater. Interfaces* **2013**, *5*, 7867−7874.
(22) Thielbeer, F.; Chankeshwara, S. V.; Bradley, M. *Biomacromolecules* **2011**, *12*, 4386−4391.
(23) Arshady, R. *Colloid Polym. Sci.* **1992**, *270*, 717−732.
(24) Sosnowski, S.; Feng, J.; Winnik, M. A. *J. Poly. Sci., Part A: Polym. Chem.* **1994**, *32*, 1497−1505.
(25) Sudol, S. S. E. D.; EL-Aasser, M. S. *J. Polym. Sci., Part A: Polym. Chem.* **1993**, *31*, 1393−1402.
(26) Horák, D. *Acta Polym.* **1996**, *47*, 20−28.
(27) Song, J. S.; Tronc, F.; Winnik, M. A. *J. Am. Chem. Soc.* **2004**, *126*, 6562−6563.
(28) Song, J. S.; Winnik, M. A. *Macromolecules* **2005**, *38*, 8300−8307.
(29) Würthner, F. *Chem. Commun.* **2004**, *14*, 1564−1579.
(30) Hains, A. W.; Chen, H.-Y.; Reilly, T. H., , III; Gregg, B. A. *ACS Appl. Mater. Interfaces* **2011**, *3*, 4381−4347.
(31) Singh, H.; Balamurugan, A.; Jayakannan, M. *ACS Appl. Mater. Interfaces* **2013**, *5*, 5578−5591.
(32) Kim, I.; Haverinen, H. M.; Li, J.; Jabbour, G. E. *ACS Appl. Mater. Interfaces* **2010**, *2*, 1390−1394.
(33) Bhavsar, G. A.; Asha, S. K. *Chem.—Eur. J.* **2011**, *17*, 12646−12658.
(34) Deepa, P.; Jayakannan, M. *J. Polym. Sci., Part A: Polym. Chem.* **2008**, *46*, 5897−5915.
(35) Avlasevich, Y.; Li, C.; Müllen, K. *J. Mater. Chem.* **2010**, *20*, 3814−3826.
(36) Peeters, E.; Ramos, A. M.; Meskers, S. C. J.; Janssen, R. A. J. *J. Chem. Phys.* **2000**, *112*, 9445−9454.
(37) Shim, S. E.; Yang, S.; Choi, H. H.; Choe, S. *J. Polym. Sci., Part A: Polym.Chem.* **2004**, *42*, 835−845.
(38) Goel, M.; Jayakannan, M. *J. Phys. Chem. B* **2010**, *114*, 12508−12519.
(39) Chen, Z.; Lohr, A.; Saha-Möller, C. R.; Würthner, F. *Chem. Soc. Rev.* **2009**, *38*, 564−584.
(40) Rodríguez-Abreu, C.; Aubery-Torres, C.; Solans, C.; López-Quintela, A.; Tiddy, G. J. T. *ACS Appl. Mater. Interfaces* **2011**, *3*, 4133−4141.
(41) Langhals, H.; Ismael, R.; Yürük, O. *Tetrahedron* **2000**, *56*, 5435−5441.
(42) Langhals, H.; Krotz, O.; Polborn, K.; Mayer, P. *Angew. Chem., Int. Ed.* **2005**, *44*, 2427−2428.
(43) Würthner, F.; Kaiser, T. E.; Saha-Möller, C. R. *Angew. Chem., Int. Ed.* **2011**, *50*, 3376−3410.
(44) Qu, J.; Zhang, J.; Grimsdale, A. C.; Müllen, K.; Jaiser, F.; Yang, X.; Neher, D. *Macromolecules* **2004**, *37*, 8297−8306.
(45) Zhao, Q.; Zhang, S.; Liu, Y.; Mei, J.; Chen, S.; Lu, P.; Qin, A.; Ma, Y.; Sun, J. Z.; Tang, B. Z. *J. Mater. Chem.* **2012**, *22*, 7387−7394.
(46) Che, Y.; Yang, X.; Balakrishnan, K.; Zuo, J.; Zang, L. *Chem. Mater.* **2009**, *21*, 2930−2934.
(47) Ford, W. E.; Kamat, P. V. *J. Phys. Chem.* **1987**, *91*, 6373−6380.
(48) Neuteboom, E. E.; Meskers, S. C. J.; Meijer, E. W.; Janssen, R. A. J. *Macromol. Chem. Phys.* **2004**, *205*, 217−222.
(49) Mizoshita, N.; Tani, T.; Inagaki, S. *Adv. Mater.* **2012**, *24*, 3350−3355.
(50) Schütze, F.; Stempfle, B.; Jüngst, C.; Wöll, D.; Zumbusch, A.; Mecking, S. *Chem. Commun.* **2012**, *48*, 2104−2106.